Planta (1986) 167:425–436

Planta

Immunogold localization of nodule-specific uricase in developing soybean root nodules

K.A. Van den Bosch* and E.H. Newcomb
Department of Botany, University of Wisconsin, Madison, WI 53706, USA

Abstract. Immunogold labeling was used to study the time of appearance and distribution of a nodule-specific form of uricase (EC 1.7.3.3) in developing nodules of soybean (*Glycine max* (L.) Merr.) inoculated with *Bradyrhizobium japonicum*. The enzyme was detected in thin sections of tissue embedded in either L R White acrylic resin or Spurr's epoxy resin, by employing a polyclonal antibody preparation active against a subunit of soybean nodule uricase. Antigenicity was better preserved in L R White resin, but ultrastructure was better maintained in Spurr's. Uricase was first detectable with protein A-gold in young, developing peroxisomes in uninfected cells, coincident with the release of *Bradyrhizobium* bacteroids from infection threads in adjacent infected cells. As the peroxisomes enlarged, labeling of the dense peroxisomal matrix increased. Gold particles were never observed over the paracrystalline inclusions of peroxisomes, however. Despite a close association between enlarging peroxisomes and tubular endoplasmic reticulum, uricase was not detectable in the latter. In mature nodules, labeling of uricase was limited to the large peroxisomes in uninfected cells. Small peroxisome-like bodies present in infected cells did not become labeled.

Key words: *Bradyrhizobium* – *Glycine* (uricase in nodules) – Immunogold labeling – Nodulin – Peroxisome biogenesis – Root nodules – Uricase.

Introduction

Members of the leguminous tribe Phaseoleae, including soybean, bean and cowpea, transport symbiotically fixed nitrogen from root nodules to other parts of the plant principally in the form of the ureides allantoin and allantoic acid (Pate 1976; Herridge et al. 1978; Schubert 1981). The pathway of ureide synthesis described for soybean (Reynolds et al. 1982) and cowpea (Shelp et al. 1983) involves the de-novo synthesis of purines from amino acids and the oxidation of purines to form ureides.

The enzyme uricase (EC 1.7.3.3) is near the end of this pathway and is responsible for the breakdown of uric acid, the product of purine catabolism, to allantoin (Hanks et al. 1981). Recently, a nodule-specific protein from soybean, nodulin-35, has been identified as a 33-kdalton (kDa) subunit of uricase (Bergmann et al. 1983). The nodulins are nodule-specific, plant-encoded proteins that are synthesized only during symbiosis (Legocki and Verma 1980); they are not found in other plant organs. Nodulin-35, one of the most abundant proteins in mature soybean nodules, is believed to be responsible for the large increase in uricase activity which occurs in nodules following the onset of nitrogenase activity (Bergmann et al. 1983).

Uricase is sometimes found along with catalase in peroxisomes in plant and animal tissues (see reviews by Beevers 1979; Lazarow 1981). The presence of numerous enlarged peroxisomes in uninfected cells of the central infected zone of soybean nodules led Newcomb and Tandon (1981) to predict that the last steps of ureide synthesis would be found to take place in these cells. This prediction was borne out in subsequent biochemical studies on separated infected and uninfected cells. Hanks et al. (1983), in particular, found most of the uricase and allantoinase activities in the fractions from uninfected cells. It was unclear from their results, however, whether a small amount of ureide formation might not also occur in the infected cells. Furthermore, Newcomb et al. (1985) have reported that infected cells contain small peroxisome-like bodies that could conceivably func-

* To whom correspondence should be addressed

Abbreviations: BSA = bovine serum albumin; Da = dalton; ER = endoplasmic reticulum; IgG = immunoglobulin G

tion in the production of ureides. A method capable of demonstrating the presence of uricase and allantoinase in situ is needed if the cellular and subcellular location of these enzymes is to be determined unambiguously.

Several approaches have now been used to localize enzymes that catalyze the last few steps in ureide formation in soybean nodules. Catalase has been localized in the peroxisomes of uninfected cells by means of ultrastructural cytochemistry employing 3,3′-diaminobenzidine (Marks and Sprent 1974; Newcomb and Tandon 1981; Newcomb et al. 1985), while uricase has been localized by Verma and associates with two different immunological procedures. The presence of uricase in the uninfected cells was demonstrated using immunofluorescence (Bergmann et al. 1983), while the localization of the same enzyme in the peroxisomes of these cells was achieved with immunogold labeling, which affords a higher level of resolution (Nguyen et al. 1985).

In the work reported here, we have made use of the immunogold technique to follow the time of appearance of nodule-specific uricase in peroxisomes and possibly in other subcellular structures in differentiating nodules. We believe this developmental study is the first to correlate the induction of a nodulin with morphological events. Two further goals of the study were 1) to optimize procedures that preserve both ultrastructural detail and high antigenicity in the immunogold labeling of uricase, and 2) to determine whether uricase is demonstrable in the small peroxisomes of the infected cells using the immunogold technique.

Material and methods

Plants. Seeds of soybean (*Glycine max* (L.) Merr. cv. Evans; Olds Seed Co., Madison, Wis., USA) were inoculated with *Bradyrhizobium japonicum* strain USDA 3I1B110 (Nitragin Co., Milwaukee, Wis., USA). The seeds were sown in a vermiculite/perlite (Strong-lite Products, De Kalb, Ill., USA) mixture (50/50, v/v) and grown under greenhouse conditions. Seedlings were watered twice weekly with a modified Hoagland's solution minus nitrogen (0.25-strength of the solution of Hoagland and Snyder 1933; with equivalent amounts of the chloride salts of calcium and potassium added in place of $Ca(NO_3)_2$ and KNO_3).

Specimen preparation. For examination of mature nodules, the nodules were collected three to five weeks after seeds were inoculated and sown. For a developmental study, nodules were excised from the top 2.5 cm of primary roots of seedlings 8, 10, 12 and 14 d after the seeds had been inoculated and sown. Nodules were first macroscopically visible on day 8. Smaller nodules were fixed whole while larger nodules were sliced into the fixative. The larger nodules were sliced longitudinally in half or into sections about 1 mm thick, depending on their size. Fixation was carried out in 3% glutaraldehyde in 50 mM potassium-phosphate buffer, pH 6.8, for 1.5 h at room temperature. Specimens were washed in phosphate buffer and post-fixed for 2 h in 2% osmium tetroxide in the same buffer. Nodules were either dehydrated in an acetone series (10, 30, 50, 70, 95, 100%) and embedded in Spurr's epoxy resin (Spurr 1969), or dehydrated in an ethanol series (10, 30, 50, 70, 95, 100%) and embedded in L R White acrylic resin (purchased from the London Resin Company through Ernst Fullam, Latham, N.Y., USA). Polymerization of L R White was effected by heat-curing the resin at 55° C for 24 h. Thin sections, silver-gold in color, were collected on uncoated gold or nickel grids. In preliminary experiments it was observed that background labeling was greatly reduced on uncoated grids compared to carbon- and formvar-coated grids. Sections adhered better if the grids were washed in 10% formic acid, followed by water and acetone rinses, prior to use.

Immunolabeling. Antibodies against nodulin-35, the 33-kDa subunit of nodulin-specific uricase, were a gift from D.P.S. Verma (McGill University, Montreal, P.Q., Canada) and were raised in rabbits as described in Bergmann et al. (1983). Prior to labeling, sections on grids were treated with aqueous sodium *meta*periodate for 1 h in order to overcome the masking of antigenic sites by osmium (Bendayan and Zollinger 1983; Craig and Goodchild 1984). A 0.56 M solution (Doman and Trelease 1985) was used instead of a saturated solution to avoid the precipitation of periodate on grids. Following the periodate pretreatment, sections on grids were placed in 1% (w/v) bovine serum albumin (BSA) in TBST buffer (Tris-buffered saline plus Tween, containing 10 mM 3-amino-2-(hydroxymethyl)-1,3-propanediol [Tris]-HCl, pH 7.2, 500 mM NaCl and 0.3% (v/v) Tween-20 [polyoxyethylenesorbitan monolaurate; Sigma Chemical Co., St. Louis, Mo., USA]). The grids were then immersed in anti-soybean nodulin-35 diluted to a concentration of 30–60 µg immunoglobulin G (IgG)/ml in 1% BSA in TBST. After incubation for 1 h in the antibody preparation, the grids were washed in TBST and transferred to TBST containing protein A-gold (20 nm in diameter). Protein A-gold, a gift from D.E. Titus (University of Wisconsin, Madison), was prepared as described in Titus and Becker (1985). After 30 min, grids were washed first in TBST, then in filtered distilled water, and blotted dry. Control experiments included substitution of TBST or pre-immune IgG for anti-nodulin-35. Sections were post-stained in 2% aqueous uranyl acetate for 10 min and in lead citrate (Reynolds 1963) for 5 min before observation in a Hitachi (Tokyo, Japan) H-600 electron microscope operated at 75 kV.

Quantification of labeling. In order to quantify the amount of labeling, gold particles over profiles of peroxisomes, plastids, mitochondria and bacteroids were counted in ten micrographs per treatment. Gold particles over the cytoplasm exclusive of these organelles were counted for the entire area of each micrograph. Negatives taken at an original magnification of ×12000 were projected on a photographic enlarger to a total magnification of ×33000. Profile area was estimated using Weibel's point-count method (Weibel 1979, Chpt. 4); density of labeling was expressed as number of gold particles per μm^2 of profile area.

Results

Preservation of antigenicity and ultrastructural quality. Soybean nodules embedded in either Spurr's epoxy resin (Fig. 1) or L R White acrylic

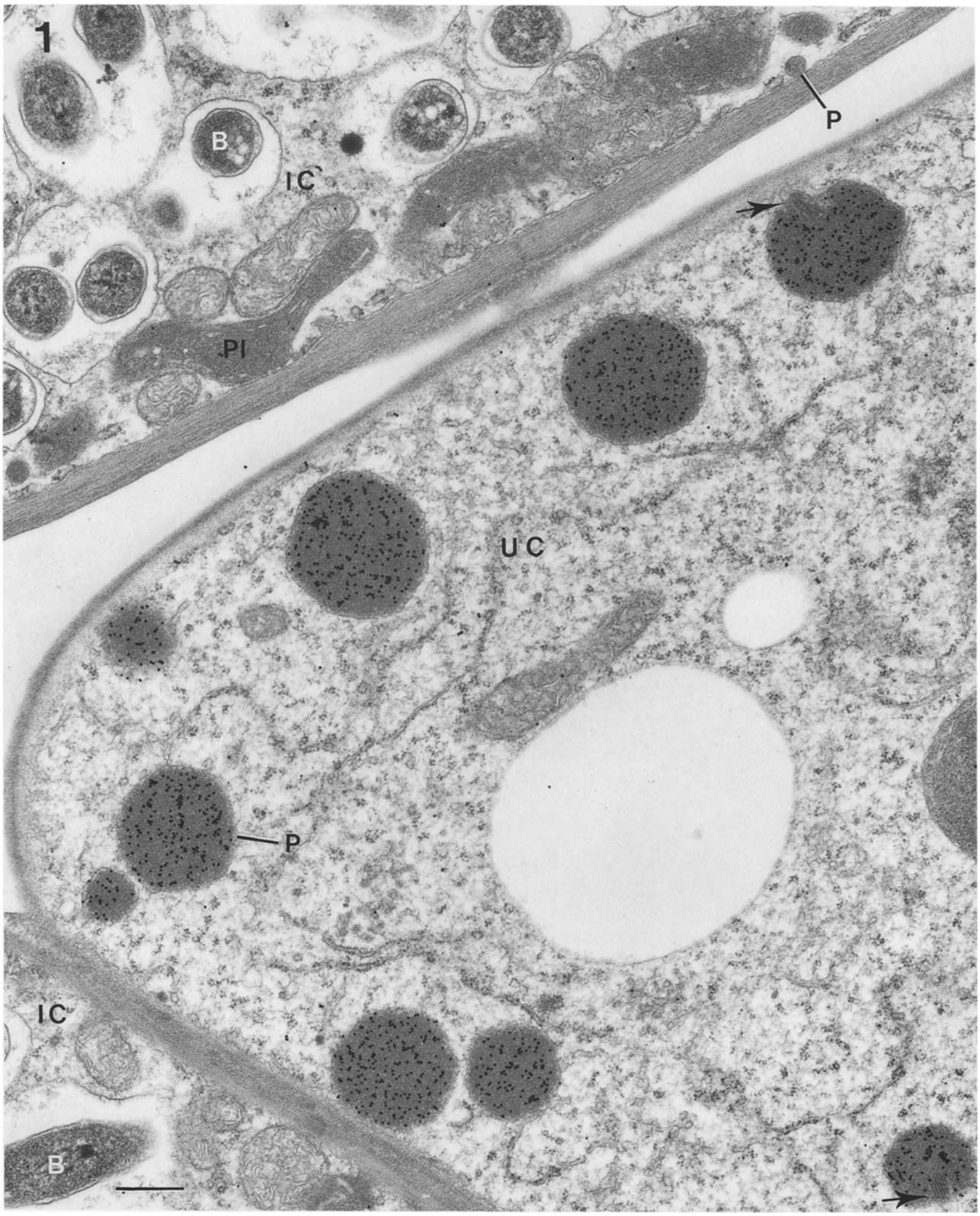

Fig. 1. Soybean nodule excised from a three-week-old plant, embedded in Spurr's resin and labeled with anti-uricase, followed by protein A-gold. Only large peroxisomes in uninfected cells are labeled. Note paracrystalline material (*arrows*) in two peroxisomes. ×24000; bar = 0.5 μm

Abbreviations used in figures: *B*, *Bradyrhizobium* bacteroid; *CER*, cisternal endoplasmic reticulum; *IC*, infected cell; *IT*, infection thread; *P*, peroxisome; *Pl*, plastid; *TER*, tubular endoplasmic reticulum; *UC*, uninfected cell

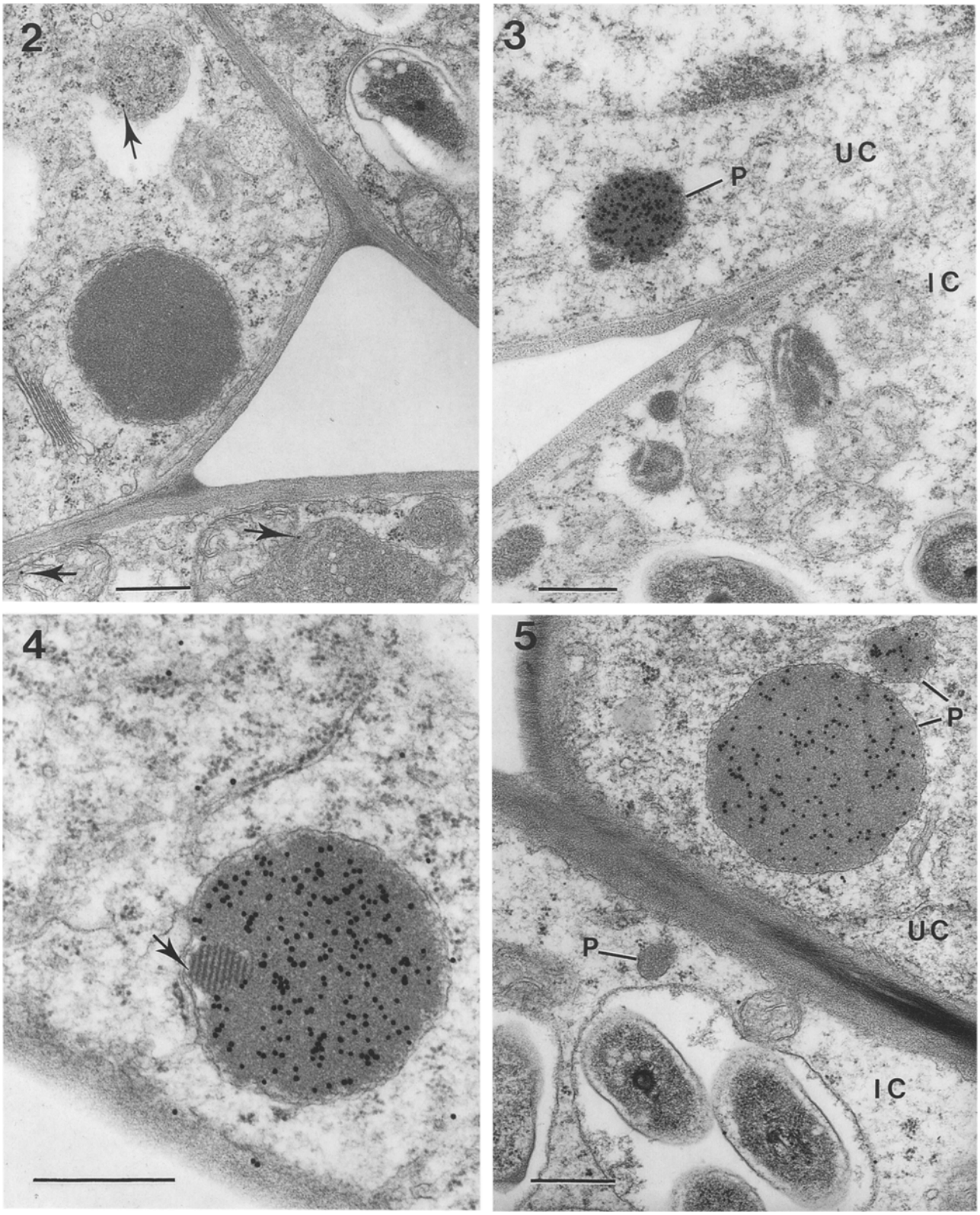

Fig. 2. Soybean nodule 21 d after inoculation, embedded in Spurr's resin. Section was incubated in pre-immune serum, followed by protein A-gold. Only a few gold particles (*arrows*) are present. Note that peroxisome is not labeled. × 26000; bar = 0.5 μm

Fig. 3. Soybean nodule 14 d after inoculation, embedded in L R White and labeled with anti-uricase followed by protein A-gold. Peroxisome in uninfected cell shows heavy labeling. × 27000; bar = 0.5 μm

resin (Fig. 3) retained a high degree of protein antigenicity and exhibited a low amount of background labeling. Of the two resins, L R White was superior in maintaining antigenicity. In two separate experiments where labeling was quantified, sections of soybean nodule in L R White showed more than twice the number of gold particles (2.13× and 2.09× as many) per peroxisome profile as did material in Spurr's resin.

Ultrastructural preservation of cellular detail was excellent with both types of resin before treatment with sodium metaperiodate. However, sections of tissue in L R White suffered some loss of membrane contrast after incubation in periodate, which made it difficult to discern membranous structures such as smooth endoplasmic reticulum (ER) and Golgi and lessened the resolution of the technique. Bleaching of membranes was not observed in Spurr's-embedded material, which therefore gave more faithful ultrastructural preservation when immunolabeled with protein A-gold.

Substitution of pre-immune IgG for anti-uricase IgG resulted in the binding of very few gold particles on either Spurr's or L R White sections. Material embedded in Spurr's and incubated in pre-immune IgG is illustrated in Fig. 2. No labeling at all occurs in the peroxisome. Elimination of the antibody incubation step similarly resulted in very low background labeling, resembling the control pictured in Fig. 2 (not illustrated).

Immunolabeling of mature nodules. Figures 1, 4 and 5 are representative views of nodule tissue from three-week-old plants following labeling with antibodies specific for the 33-kDa subunit of nodule-specific uricase. Heavy labeling for uricase occurs over the large peroxisomes in uninfected cells. Within these peroxisomes, the matrix is uniform and completely fills the organelle. Gold particles appear to be uniformly distributed over the matrix. Regions of paracrystalline protein present in some peroxisome profiles (Figs. 1, 4) do not become labeled for uricase using immunogold labeling techniques.

Small peroxisome-like bodies are seen occasionally in the peripheral cytoplasm of infected cells in Spurr's-embedded material (Figs. 1, 5); peroxisomes in infected cells cannot be distinguished from small plastid profiles in L R White-embedded material because of membrane bleaching. Gold particles occur infrequently over these putative peroxisomes, with a labeling density resembling that over other organelles and the cytoplasm (Table 1). Labeling of peroxisome profiles in infected cells therefore appears not to be above the level of background labeling, allowing us to conclude that uricase is not present in these organelles at a level sufficient to be detectable with our technique.

Table 1. Immunolabeling of uricase in infected and uninfected cells of soybean nodules embedded in Spurr's resin

Structure	No. of profiles counted	Gold particles per $\mu m^2 \pm$ SE
Peroxisomes in uninfected cells	23	125.5±5.7
Peroxisomes in infected cells	20	1.5±1.1
Plastids	27	1.2±0.4
Mitochondria	39	0.3±0.2
Bradyrhizobium bacteroids	31	2.1±0.6
Cytoplasm of uninfected cells	10[a]	0.6±0.1
Cytoplasm of infected cells	10[a]	0.8±0.2

[a] See *Material and methods* for details

Appearance of uricase in developing nodules. The observations on developing nodules cover the 8th through the 14th day after inoculation, a 7-d period during which the infection threads grow and branch, the rhizobia escape from the threads, and then (as bacteroids enclosed in membrane-bounded sacs) multiply rapidly in the cytoplasm of the host cells. Light micrographs of median sections through nodules harvested 8, 10, 12 and 14 d after inoculation are illustrated in Fig. 6. At 8 d, the central tissue of the nodule is composed of densely cytoplasmic meristematic cells. Infection threads are visible in some cells. By 10 d, uninfected cells are visible as files of vacuolate cells distributed through the dense mass of the larger, darkly stained infected cells. The uninfected cells and more rapidly enlarging infected cells are readily distinguished from one another after 12 d. On the 14th day, cell enlargement and nodule growth are still taking place.

Fig. 4. Peroxisome in uninfected cell of a soybean nodule in Spurr's-embedded material labeled with anti-uricase and protein A-gold. Note that paracrystalline region (*arrow*) of the peroxisome is not labeled. ×49000; bar = 0.5 μm

Fig. 5. Portions of infected and uninfected cells from a soybean nodule 21 d after inoculation. Specimen was embedded in Spurr's resin, labeled with anti-uricase, followed by protein A-gold. Note the difference in intensity of labeling over the peroxisomes in the infected and uninfected cells. ×29000; bar = 0.5 μm

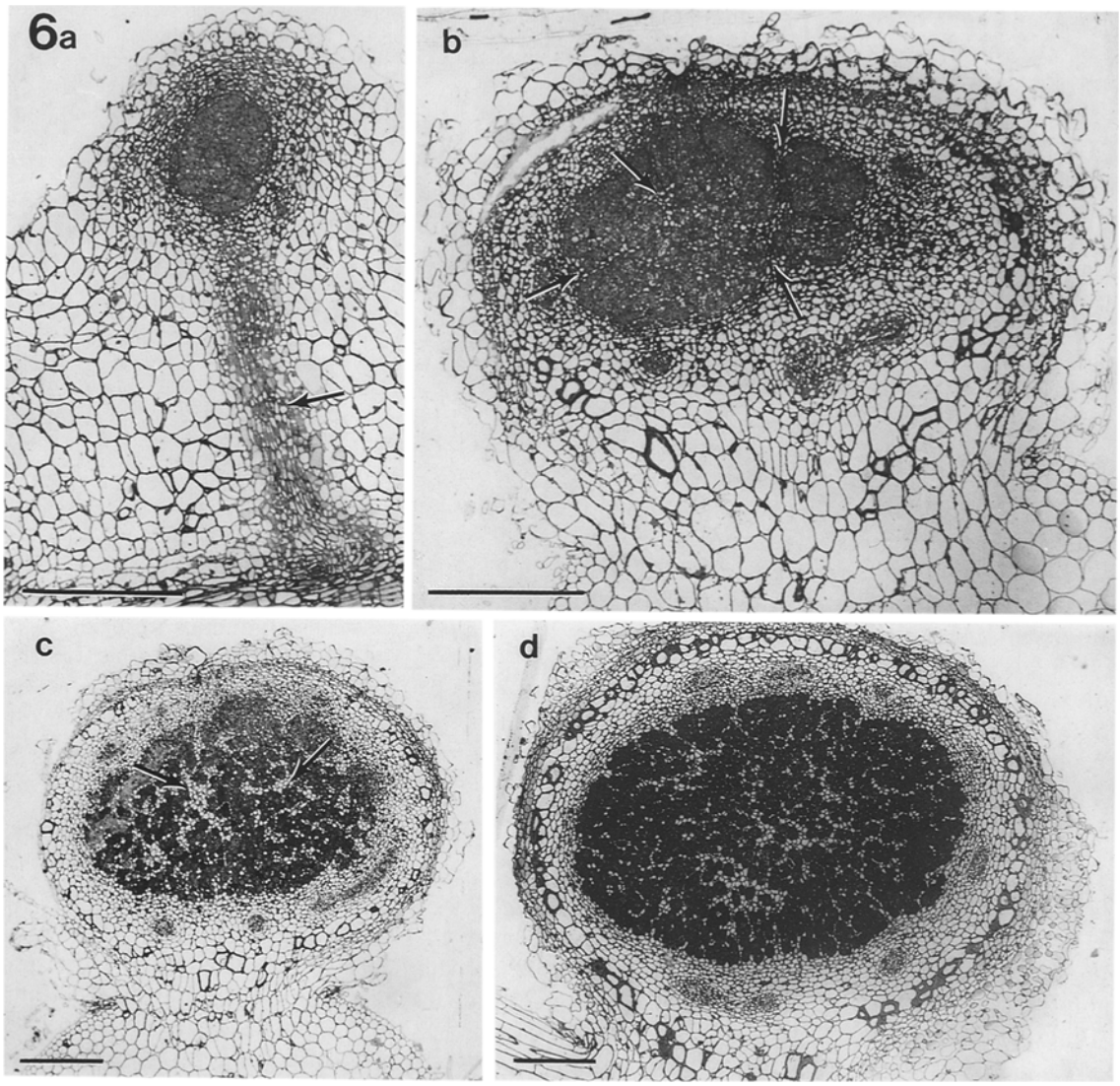

Fig. 6a–d. Light micrographs of longitudinal sections of developing soybean nodules. All bars = 250 μm. **a** Nodule 8 d after inoculation. *Arrow* indicates developing vascular strand which connects the nodule to the root vasculature. ×86. **b** 10 d. *Arrows* indicate regions of developing uninfected cells. ×86. **c** 12 d. *Arrows* indicate uninfected cells. ×45. **d** 14 d. ×45

At the earliest stage studied here (8 d after planting under our growth conditions), when infection threads have penetrated the host cells but the rhizobia have not yet been released, it is impossible to distinguish ultrastructurally between those cells that will and those that will not become infected. The cells are meristematic in appearance and contain a sparse population of small peroxisomes that resemble those of meristematic cells generally. These peroxisomes fail to become labeled for uricase (not illustrated).

Differentiating peroxisomes in uninfected cells are first detectable in nodules on 10-d-old plants, corresponding approximately with the release of bacteroids in adjacent infected cells (Fig. 7). Although gold particles are present over most of these small peroxisomes (Fig. 7a, b), not all profiles at this stage are labeled (Fig. 7c). The pattern of labeling is similar in the two resins. Within a peroxisome, the central dense matrix is labeled, but the peripheral, more electron-transparent region usually is not. Like the paracrystalline regions in older peroxisomes, the paracrystalline material frequently seen in young peroxisomes is not labeled.

During the early stages of nodule development, dilated ER tubules containing flocculent material are often observed surrounding and sometimes apparently opening into the enlarging peroxisomes. Gold particles are only infrequently observed over these dilated tubules (Fig. 7d, e) despite the close

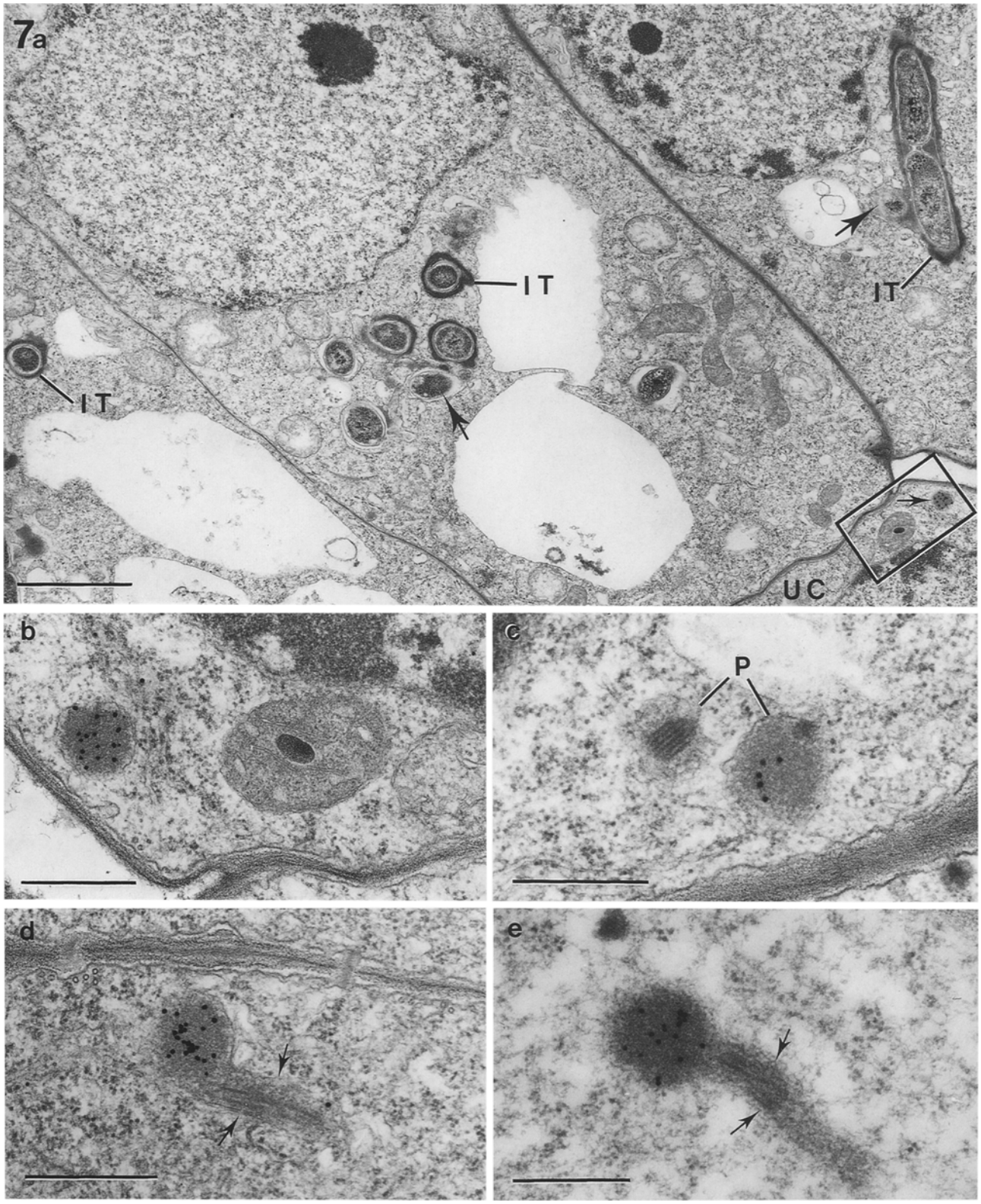

Fig. 7a–e. Electron micrographs of soybean nodules 10 d after inoculation. All views except **e** are of Spurr's-embedded material labeled with anti-uricase and protein A-gold. **a** Portions of three infected cells and one uninfected. Rhizobia (*large arrows*) are being released from infection threads. A labeled peroxisome (*small arrow*) is visible in the uninfected cell. The *boxed region* is shown enlarged in view **b**. ×9800; bar = 2.0 μm. **b** ×38000; bar = 0.5 μm. **c** Two peroxisomes in an uninfected cell. Note paracrystalline material in the *left* peroxisome. ×47000; bar = 0.5 μm. **d** Labeled peroxisome with attached dilated tubule (*arrows*). ×39000; bar = 0.5 μm. **e** View of peroxisome in L R White-embedded material, labeled as above. Note lack of label in attached dilated tubule (*arrows*). ×45000; bar = 0.5 μm

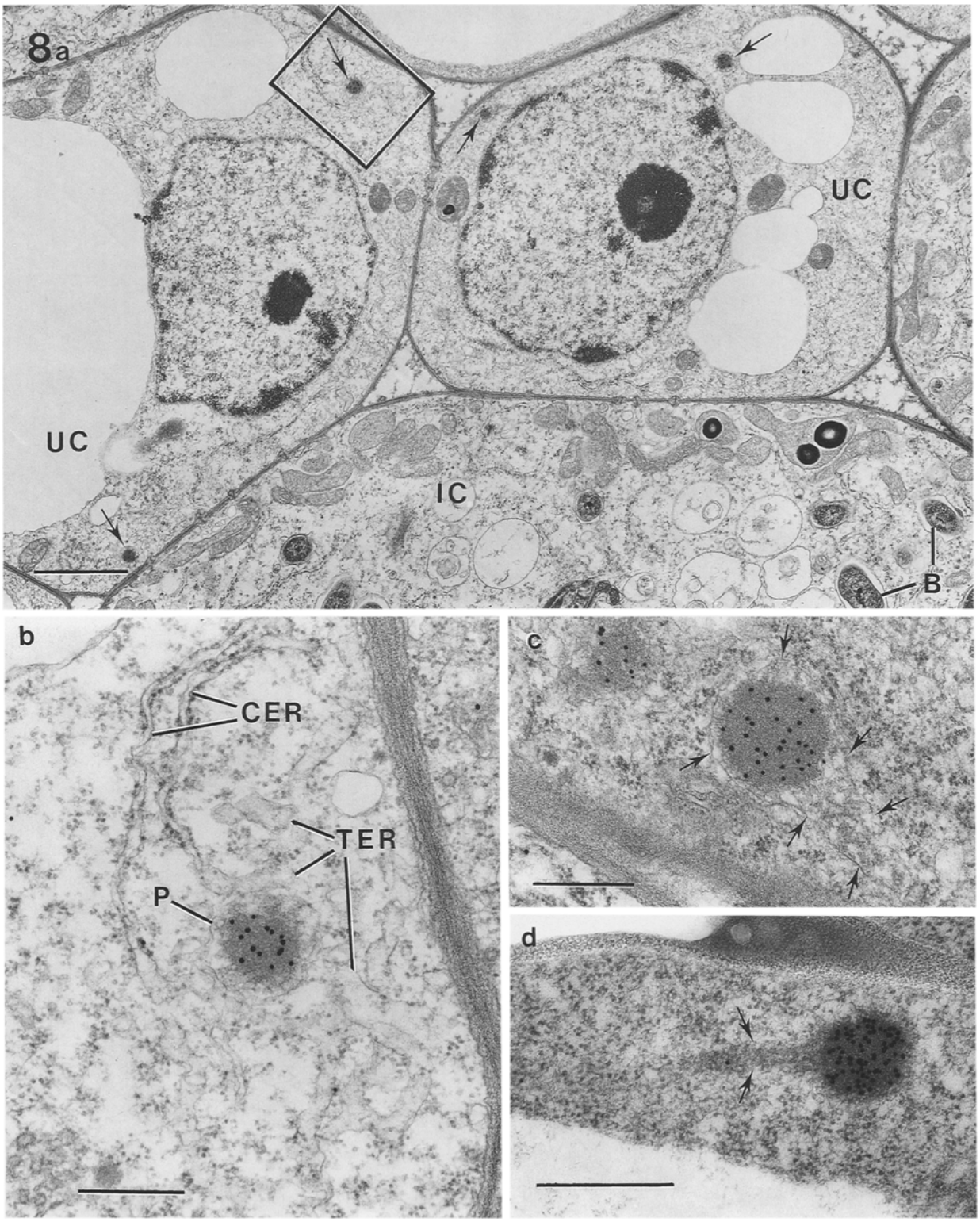

Fig. 8a–d. Electron micrographs of soybean nodules 12 d after inoculation. All views except **d** are of Spurr's-embedded material labeled with anti-uricase and protein A-gold. **a** Portions of several infected and uninfected cells. Note *Bradyrhizobium* bacteroids in infected cells and developing peroxisomes (*arrows*) in uninfected cells. ×7900; bar=2.0 μm. *Boxed region* is shown enlarged in view **b**. **b** Developing peroxisome with associated tubular ER. Note that tubular ER is continuous with cisternal ER. ×36000; bar=0.5 μm. **c** Two peroxisomes in uninfected cell. *Arrows* indicate membrane bounding peroxisome and attached tubule. ×34400; bar=0.5 μm. **d** Labeled peroxisome from L R White-embedded material, labeled as above. *Arrows* indicate attached tubule. ×46000; bar=0.5 μm

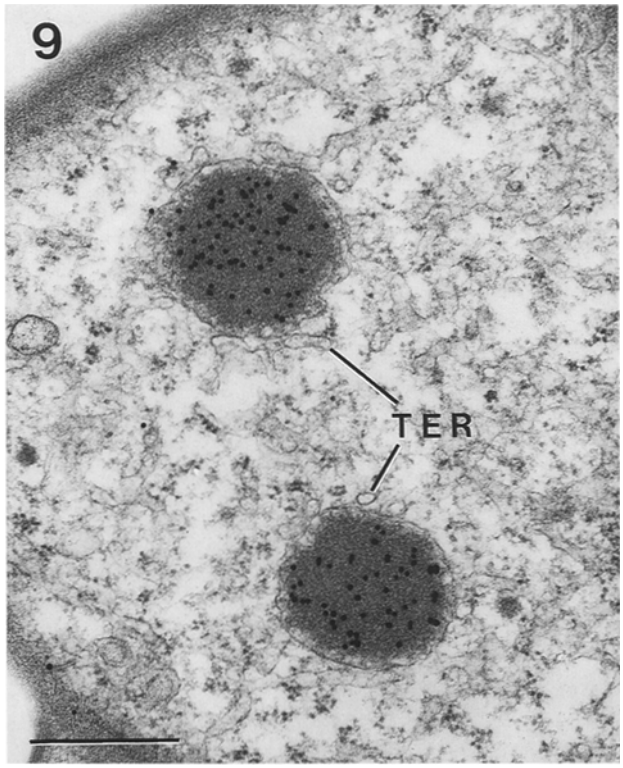

Fig. 9. View of Spurr's embedded soybean nodule 14 d after inoculation. Label for uricase does not occur over tubular endoplasmic reticulum. ×41000; bar=0.5 μm

association between the tubules and peroxisomes and the similarity in appearance of their contents. Similarly, labeling for uricase is not detectable over other regions of the ER, over free polysomes, or elsewhere in the cytoplasm (Fig. 7b–d).

By the 12th day after planting, the bacteroids have become more numerous in the infected cells (Fig. 8a), while the peroxisomes in the uninfected cells have become larger and more heavily labeled than at 10 d (Fig. 8b–d). By this stage also, tubular ER has become a more prominent cellular component of the uninfected cells. At 14 d, the peroxisomes of the uninfected cells are still enlarging and accumulating matrix material. Tubular ER is most abundant at this stage and is closely associated with developing peroxisomes (Fig. 9). As found for younger material, at both 12 and 14 d, gold particles occur infrequently over the ER. Embedments in Spurr's and L R White give similar results, although the labeling is heavier with L R White.

Discussion

Localizing the enzymes of the ureide pathway and correlating their appearance with other developmental changes in the nodule pose special problems because the pathway is distributed between two different, intermingled cell types. Immunocytochemistry, as applied in the present study by immunogold labeling, is especially well suited for this type of investigation. No disruption of tissue is required, since the procedures are carried out on fixed, embedded and thin-sectioned material. Furthermore, the technique combines the specificity of an immunological reaction with the high resolution afforded by the electron microscope.

Biochemical fractionation procedures, on the other hand, involve incomplete cell separation followed by cell disruption, hence may not permit differentiating between similar components derived from two different cell types. In enzyme assays carried out on separated infected and uninfected cells from soybean nodules, Hanks et al. (1983) determined that the uninfected cell fraction contained most of the activity of catalase, uricase and allantoinase. However, because of cross-contamination between the two fractions, it was not possible to determine whether uricase was completely absent from the infected cells. Shelp et al. (1983), using similar techniques on nodules of cowpea, also a ureide transporter, found several enzymes of the ureide pathway distributed through both infected and uninfected cells and also the cortex, indicating considerable cross contamination between fractions. Homogenization procedures can also damage cellular components, releasing soluble proteins. For example, Hanks et al. (1981) could find only about 15% of the total uricase activity in the peroxisomal fraction following differential centrifugation, presumably because of the fragile nature of these organelles.

Modifying tissue treatment to improve the results of immunogold labeling. Successful application of immunogold labeling techniques, as developed by Roth et al. (1978), requires good preservation of both structural detail and antigenicity in embedded material. An osmium post-fixation step, conventionally used to preserve and stain membranes, was avoided in the early work on immunolabeling (Roth 1983) because it was believed that it destroyed antigenicity. However, Bendayan and Zollinger (1983) discovered that osmium masks rather than destroys antigenicity, and that antigenic sites on the surface of thin sections can be unmasked by incubating specimens in a sodium *meta*periodate solution. Periodate treatment thus permits good immunolabeling of material in which the membranes have been well preserved, although it is not successful with all antigens (Brewin et al. 1985).

Immunogold labeling of material post-fixed with osmium has been performed on specimens embedded both in epoxy resins and in L R White, a polar acrylic resin. Craig and Miller (1984) have reported improved labeling with L R White, compared to epoxy resin. In our study, tissue embedded in L R White was labeled about twice as heavily as material in Spurr's resin. However, following periodate treatment, membranes of specimens in L R White had a bleached appearance and were difficult to resolve. This indicates that neither procedure represents an ideal compromise between preservation of ultrastructural detail and antigenicity, and that conclusions should be drawn based on examination of material treated in more than one way.

Time of appearance of nodule-specific uricase during nodule development. The several known nodulins are expressed at different times during nodule development. While certain nodulins are induced during early stages of the symbiotic interactions (Bisseling et al. 1983; Fuller and Verma 1984), the appearance of others may coincide with leghemoglobin expression (Bisseling et al. 1983; Verma et al. 1984) just prior to the onset of nitrogenase activity (Bisseling et al. 1980; Verma et al. 1979, 1981). Nodulin proteins and nodule-specific mRNA sequences from extracts of developing nodules have been studied, but information about the expression of a nodulin as tissue differentiation proceeds has not been reported.

We find that uricase (nodulin-35; Bergmann et al. 1983) is expressed in uninfected cells only after they have become recognizably different from the infected cells in their ultrastructure. Immunogold labeling first detects the presence of uricase in uninfected cells coincident with the infection of neighboring cells through the release of *Bradyrhizobium* bacteroids from infection threads. Prior to bacteroid release, the two cell types are indistinguishable.

It is not yet known why some cells become infected and others remain uninfected. We occasionally observe infection threads in fully differentiated uninfected cells, so it is evident that their presence alone does not guarantee infection. It seems clear, though, that developmental events in infected and uninfected cells are closely coordinated. Uricase and peroxisome biogenesis are induced only in cells which escape infection; nevertheless, the protein appears only after neighboring cells have become infected.

The mode of induction of uricase in uninfected cells is unknown, but it appears to be unrelated to the availability of uric acid in the cells. Several lines of evidence indicate that the expression of uricase is independent of nitrogenase activity, upon which formation of uric acid is dependent. Both mRNA coding for nodule-specific uricase (Nguyen et al. 1985) and the protein itself appear early in nodule development, although the enzyme does not reach full activity until after nitrogenase activity commences in soybean (Bergmann et al. 1983) and cowpea (Atkins et al. 1984). Moreover, uricase occurs in soybean nodules induced by ineffective strains of *Bradyrhizobium* (Legocki and Verma 1979) and in cowpea nodules grown in the absence of N_2 (Atkins et al. 1984).

Labeling of uricase during peroxisome biogenesis. Nguyen et al. (1985) have recently demonstrated that nodulin-35 mRNA is translated on free polysomes and that the peptide lacks a signal sequence, implying that it is not processed co-translationally into the ER lumen. Our results are consistent with these findings, indicating that uricase subunits are taken up post-translationally directly into developing peroxisomes, as has been demonstrated for rat-liver uricase and catalase (Goldman and Blobel 1978). Uricase has not been detected on polysomes or in the cytoplasm in our work, nor in immunogold studies of other plant peroxisomal enzymes (Doman and Trelease 1985; Titus and Becker 1985). The amounts of these proteins at their site of synthesis are probably too small to be detected.

It has been suggested (Newcomb et al. 1985) that the tubular ER may play a role in the biogenesis of nodule peroxisomes because it proliferates and frequently envelopes the peroxisomes during the stage when they are increasing in size and matrix density. It is possible that uricase subunits might be taken up post-translationally into the tubular ER and transported to young peroxisomes. However, our failure to detect uricase in any portion of the ER with the immunogold technique, while not conclusive, does not support the idea that tubular ER serves as a conduit for uricase to the developing peroxisomes. By contrast, proteins which are cotranslationally processed and transported via the ER to developing organelles have been clearly detected in the ER cisternae using techniques similar to those reported here (Craig and Goodchild 1984; Craig and Miller 1984; Bendayan and Zollinger 1983).

Distribution of uricase in mature nodules. The application of immunogold techniques for ultrastructural localization has confirmed the presence of uri-

case in the enlarged peroxisomes of uninfected cells (Nguyen et al. 1985). However, small peroxisome-like bodies occur at roughly the same frequency in infected cells as do peroxisomes in uninfected cells (Newcomb et al. 1985). Based on the much greater total volume and the matrix density of peroxisomes in uninfected cells, Newcomb et al. (1985) suggested that these cells are responsible for virtually all of the uricase activity. Using immunogold techniques, we have now demonstrated that nodule-specific uricase cannot be detected in the peroxisomes of infected cells, when the same techniques result in heavy labeling of peroxisomes in uninfected cells. The results indicate that uricase has not been expressed in the infected cells.

The labeling of mature peroxisomes in the uninfected cells indicates that uricase is distributed throughout the granular matrix. However, the crystalloid inclusions are not labeled. The frequency with which these inclusions are encountered in thin sections indicates that there may be at least one in each nodule peroxisome. Likely explanations for their lack of labeling include the possibility 1) that the crystals do not contain uricase, or 2) that the inclusions are composed of uricase, but in the paracrystalline state the antigenic sites are blocked and cannot bind with the antibodies. Although catalase is also a major component of these peroxisomes (Newcomb et al. 1985), the lattice structure of the paracrystalline regions in question does not resemble that of paracrystalline catalase within plant peroxisomes (Frederick and Newcomb 1969). The presence of paracrystalline uricase in plant peroxisomes has not been demonstrated conclusively (see Huang et al. 1983, pp. 27–31). These inclusions merit further study.

The uninfected cells in the infected region of soybean nodules are now firmly established as the site of the final steps in ureide production. However, the respective contributions of infected and uninfected cells to the earlier steps in the metabolism of recently fixed nitrogen, especially those of purine synthesis and oxidation, remain unclear (Schubert and Boland 1984). Investigation of key enzymes in this pathway by means of immunogold labeling techniques should help greatly to resolve the uncertainties.

We thank David Titus for advice on immunogold methods, and the Nitragin Company for a gift of *Bradyrhizobium* inoculum. This work was supported in part by the U.S. Department of Agriculture under Grant No. 85-CRCR-1-1619 from the Competitive Research Grants Office, and by a grant from the McKnight Foundation of Minneapolis, Minn., USA.

References

Atkins, C.A., Shelp, B.J., Storer, P.J., Pate, J.S. (1984) Nitrogen nutrition and the development of biochemical functions associated with nitrogen fixation and ammonia assimilation of nodules on cowpea seedlings. Planta **162**, 327–333

Beevers, H. (1979) Microbodies in higher plants. Annu. Rev. Plant Physiol. **30**, 159–197

Bendayan, M., Zollinger, M. (1983) Ultrastructural localization of antigenic sites on osmium-fixed tissues applying the protein A-gold technique. J. Histochem. Cytochem. **31**, 101–109

Bergmann, H., Preddie, E., Verma, D.P.S. (1983) Nodulin-35: a subunit of specific uricase (uricase II) induced and localized in the uninfected cells of soybean nodules. EMBO J. **2**, 2333–2339

Bisseling, T., Been, C., Klugkist, J., Van Kammen, A., Nadler, K. (1983) Nodule-specific host proteins in effective and ineffective root nodules of *Pisum sativum*. EMBO J. **2**, 961–966

Bisseling, T., Moen, A.A., Van den Bos, R.C., Van Kammen, A. (1980) The sequence of appearance of leghaemoglobin and nitrogenase components I and II in root nodules of *Pisum sativum*. J. Gen. Microbiol. **118**, 377–381

Brewin, N.J., Robertson, J.G., Wood, E.A., Wells, B., Larkins, A.P., Galfre, G., Butcher, G.W. (1985) Monoclonal antibodies to antigens in the peribacteroid membrane from *Rhizobium*-induced root nodules of pea cross-react with plasma membranes and Golgi bodies. EMBO J. **4**, 605–611

Craig, S., Goodchild, D.J. (1984) Periodate-acid treatment of sections permits on-grid immunogold localization of pea seed vicilin in ER and golgi. Protoplasma **122**, 35–44

Craig, S., Miller, C. (1984) L R White resin and improved on-grid immunogold detection of vicilin, a pea storage protein. Cell Biol. Int. Rep. **8**, 879–886

Doman, D.C., Trelease, R.N. (1985) Protein A-gold immunocytochemistry of isocitrate lyase in cotton seeds. Protoplasma **124**, 157–167

Frederick, S.E., Newcomb, E.H. (1969) Cytochemical localization of catalase in leaf microbodies (peroxisomes). J. Cell Biol. **43**, 343–353

Fuller, F., Verma, D.P.S. (1984) Appearance and accumulation of nodulin in mRNAs and their transcripts and their relationships to effectiveness of root nodules. Plant Mol. Biol. **3**, 21–28

Goldman, B.M., Blobel, G. (1978) Biogenesis of peroxisomes: Intracellular site of synthesis of catalase and uricase. Proc. Natl. Acad. Sci. USA **75**, 5066–5070

Hanks, J.F., Schubert, K., Tolbert, N.E. (1983) Isolation and characterization of infected and uninfected cells from soybean nodules. Plant Physiol. **71**, 869–873

Hanks, J.F., Tolbert, N.E., Schubert, K.R. (1981) Localization of enzymes of ureide biosynthesis in peroxisomes and microsomes of nodules. Plant Physiol. **68**, 65–69

Herridge, D.F., Atkins, C.A., Pate, J.S., Rainbird, R.M. (1978) Allantoin and allantoic acid in the nitrogen economy of the cowpea. Plant Physiol. **62**, 495–498

Hoagland, D.R., Snyder, W.C. (1933) Nutrition of strawberry plant under controlled conditions. Proc. Am. Soc. Hort. Sci. **30**, 288–294

Huang, A.H.C., Trelease, R.N., Moore, T.S. (1983) Plant peroxisomes. Academic Press, New York London

Lazarow, P.B. (1981) Functions and biogenesis of peroxisomes, 1980. In: International cell biology 1980–1981, pp. 633–639, Schweiger, H.G., ed. Springer, Berlin Heidelberg New York

Legocki, R.P., Verma, D.P.S. (1979) A nodule-specific plant protein (Nodulin-35) from soybean. Science **205**, 190–193

Legocki, R.P., Verma, D.P.S. (1980) Identification of "nodule-

specific" host proteins (nodulins) involved in the development of *Rhizobium*-legume symbiosis. Cell **20**, 153–163

Marks, I., Sprent, J.I. (1974) The localization of enzymes in fixed sections of soybean root nodules by electron microscopy. J. Cell Sci. **16**, 623–637

Newcomb, E.H., Tandon, S.R. (1981) Uninfected cells of soybean root nodules: ultrastructure suggests key role in ureide production. Science **212**, 1394–1396

Newcomb, E.H., Tandon, S.R., Kowal, R.R. (1985) Ultrastructural specialization for ureide production in uninfected cells of soybean root nodules. Protoplasma **125**, 1–12

Nguyen, T., Zelechowska, M., Foster, V., Bergmann, H., Verma, D.P.S. (1985) Primary structure of the soybean nodulin-35 gene encoding uricase II localized in the peroxisomes of uninfected cells of nodules. Proc. Natl. Acad. Sci. USA **82**, 5040–5044

Pate, J.S. (1976) Transport in symbiotic systems fixing nitrogen. In: Encyclopedia of plant physiology, N.S. vol. 2: Transport in plants IIB. Tissues and organs, pp. 278–306, Lüttge, U., Pitman, M.G., eds. Springer, Berlin Heidelberg New York

Reynolds, E.S. (1963) The use of lead citrate at high pH as an electron opaque stain in electron microscopy. J. Cell Biol. **17**, 208–213

Reynolds, P.H.S., Boland, M.J., Blevins, D.G., Schubert, K.R., Randall, D.D. (1982) Enzymes of amide and ureide biogenesis in developing soybean nodules. Plant Physiol. **69**, 1334–1338

Roth, J. (1983) The protein A-gold (pAg) technique – A qualitative and quantitative approach for antigen localization on thin sections. In: Techniques in immunocytochemistry, vol. 1, pp. 107–134, Bullock, G.R., Petrusz, P., eds. Academic Press, London New York

Roth, J., Bendayan, M., Orci, L. (1978) Ultrastructural localization of intracellular antigens by the use of protein A-gold complex. J. Histochem. Cytochem. **26**, 1074–1081

Schubert, K. (1981) Enzymes of purine biosynthesis and catabolism in *Glycine max*. I. Comparison of activities with N_2 fixation and composition of xylem exudate during nodule development. Plant Physiol. **68**, 1115–1122

Schubert, K., Boland, M.J. (1984) The cellular and intracellular organization of the reactions of ureide biogenesis in nodules of tropical legumes. In: Advances in nitrogen fixation research, pp. 445–452, Veeger, C., Newton, W.E., eds. Nijhoff/Junk, The Hague Boston New York

Shelp, B.J., Atkins, C.A., Storer, P.J., Canvin, D.T. (1983) Cellular and subcellular organization of pathways of ammonia assimilation and ureide synthesis in nodules of cowpea (*Vigna unguiculata* (L.) Walp). Arch. Biochem. Biophys. **224**, 429–441

Spurr, A.R. (1969) A low-viscosity epoxy resin embedding medium for electron microscopy. J. Ultrastruct. Res. **26**, 31–43

Titus, D.E., Becker, W.M. (1985) Investigation of the glyoxysome-peroxisome transition in germinating cucumber cotyledons using double-label immunoelectron microscopy. J. Cell Biol. **101**, 1288–1299

Verma, D.P.S., Ball, S., Guérin, C., Wanamaker, L. (1979) Leghemoglobin biosynthesis in soybean root nodules. Characterization of the nascent and released peptides and the relative rate of synthesis of the major leghemoglobins. Biochemistry **18**, 476–483

Verma, D.P.S., Haugland, R., Brisson, N., Legocki, R., Lacroix, L. (1981) Regulation of the expression of leghaemoglobin genes in effective and ineffective root nodules of soybean. Biochim. Biophys. Acta **653**, 98–107

Verma, D.P.S., Lee, J., Fuller, F., Bergmann, H. (1984) Leghemoglobin and nodulin genes: Two major groups of host genes involved in symbiotic nitrogen fixation. In: Advances in nitrogen fixation research, pp. 557–564, Veeger, C., Newton, W.E., eds. Nijhoff/Junk, The Hague Boston New York

Weibel, E.R. (1979) Stereological methods, vol. 1. Academic Press, New York London

Received 4 November; accepted 11 December 1985